and E. Doherty, S. Richardson, and T. Funk (Mayo Foundation) for preparation of text and figures.

References

[1] Q. Gu and J. A. Kong, "Transient analysis of single and coupled lines with capacitively-loaded junctions," *IEEE Trans. Microwave Theory Tech.*, vol. MTT-34, pp. 952–964, Sept. 1986.
[2] E. Kuester and D. Chang, "Closed-form for the current or charge distributions on parallel strips or microstrips," *IEEE Trans. Microwave Theory Tech.*, vol. MTT-28, pp. 254–259, Mar. 1980.
[3] K. S. Olson, G. W. Pan, and B. K. Gilbert, "Comments on transient analysis of single and coupled lines with capacitively-loaded junctions," *IEEE Trans. Microwave Theory Tech.*, vol. MTT-35, pp. 929–930, Oct. 1987.
[4] J. Schutt-Aine and R. Mittra, "Analysis of pulse propagation in coupled transmission lines," *IEEE Trans. Circuits Syst.*, vol. CAS-32, pp. 1214–1219, Dec. 1985.
[5] S. Nam, H. Ling, and T. Itoh, "Time-domain method of lines applied to planar guided wave structures," *IEEE Trans. Microwave Theory Tech.*, vol. 37, pp. 897–901, May 1989.
[6] A. R. Djordjevic and T. K. Sarkar, "Analysis of time response of lossy multiconductor transmission line networks," *IEEE Trans. Microwave Theory Tech.*, vol. MTT-35, pp. 898–908, Oct. 1987.
[7] G. W. Pan, K. S. Olson, and B. K. Gilbert, "Improved algorithmic methods for the prediction of wavefront propagation behavior in multiconductor transmission lines for high frequency digital signal processors," *IEEE Trans. Computer-Aided Design*, vol. 8, pp. 608–621, June 1989.
[8] B. Rubin, "The propagation characteristics of signal lines in a mesh-plane environment," *IEEE Trans. Microwave Theory Tech.*, vol. MTT-32, pp. 522–532, May 1984.

Spectral-Domain Analysis of Shielded Microstrip Lines on Biaxially Anisotropic Substrates

T. Q. Ho and B. Beker

Abstract—**The spectral-domain technique has been extended to the study of shielded microstrip lines on biaxial substrates. The analysis simultaneously includes both dielectric and magnetic anisotropy effects. A fourth-order formulation leads to the determination of the appropriate Green's function for the structure. The characteristic equation is formed through the application of the Galerkin method to the equations resulting from the boundary conditions on the strip. Numerical results are validated against the data previously published for special isotropic and dielectrically anisotropic cases. New data on the propagation constant of the shielded microstrip with different substrate permittivities and permeabilities are presented to illustrate the effects of the material parameters on the characteristics of the microstrip line.**

I. Introduction

In recent years there has been a steadily growing interest in anisotropic materials for practical uses at millimeter-wave frequencies. The wide variety of possible applications for such media include antenna radomes, substrates for microstrip patch antennas, microwave and millimeter-wave integrated circuits (MIC's), and ferrite nonreciprocal devices. As is well known, the anisotropy in the material may occur naturally or it may be purposely implanted during the fabrication process. In either case, and in particular for MIC's, anisotropic properties of substrates must be included in the analysis, for otherwise serious errors in their design can occur.

Since the early works of Owens and Edwards [1], [2], a number of authors have developed different analytical methods for studying transmission lines on anisotropic media. Among these are Alexopolous [3], [4], Horno [5], and Koul *et al.* [6], who used the quasi-static approach to study such problems, while others, among them El-Sherbiny [7], Kobayashi [8], Yang *et al.* [9], and Krowne *et al.* [10], sought full-wave solutions. Although numerous additional works dealing with anisotropic structures are available and are well documented in the literature, the major effort thus far has been directed toward transmission lines with dielectrically anisotropic media. Until now, only a few treatments have been devoted to lines on substrates that are characterized by both $[\epsilon]$ and $[\mu]$ tensors. In one of them, Mariki *et al.* [11] applied the transmission line matrix method to analyze a shielded line on anisotropic substrate. However, no data for magnetic anisotropy effects on propagation constants were provided in that study. On the other hand, for an open structure, Tsalamengas *et al.* [12] used a semianalytical technique which can be used for substrates that are characterized by all nine elements of permittivity and permeability tensors.

In this paper, the spectral-domain method is extended to the study of shielded microstrip lines on biaxially dielectric and magnetic anisotropic substrates. The solution to Maxwell's equations, which for this problem reduces to two coupled second-order differential equations and eventually to two uncoupled fourth-order equations for two components of the electric field, leads directly to the determination of Green's function for the structure. The derivation of the characteristic equation for the propagation constant is carried out using Galerkin's technique in the Fourier domain. To demonstrate numerical efficiency of the spectral-domain approach, results for the convergence studies are included along with samples of the time required for the execution of the code. Numerical results calculated by this method for isotropic as well as dielectrically anisotropic substrates are compared with the existing data, and in both cases a very good agreement is observed. New data for the propagation constant of the shielded lines on substrates simultaneously characterized by different values of $[\epsilon]$ and $[\mu]$ are also generated.

II. Analytical Formulation

Consider the geometry shown in Fig. 1, which illustrates the cross section of the shielded microstrip line situated inside a metal housing along with the coordinate system used in the analysis. Furthermore, the cross section of the structure is assumed to be uniform in the z direction. The metal strip is taken as perfectly conducting and infinitely thin in the x direction. The lossless substrate, which has thickness h_1 and width b, is characterized by homogeneous biaxial permittivity and permeability tensors having the following forms:

$$[\epsilon] = \epsilon_0 \begin{vmatrix} \epsilon_{xx} & 0 & 0 \\ 0 & \epsilon_{yy} & 0 \\ 0 & 0 & \epsilon_{zz} \end{vmatrix} \tag{1a}$$

$$[\mu] = \mu_0 \begin{vmatrix} \mu_{xx} & 0 & 0 \\ 0 & \mu_{yy} & 0 \\ 0 & 0 & \mu_{zz} \end{vmatrix} \tag{1b}$$

Manuscript received September 26, 1990; revised January 15, 1991.
The authors are with the Department of Electrical and Computer Engineering, University of South Carolina, Columbia, SC 29208.
IEEE Log Number 9144278.

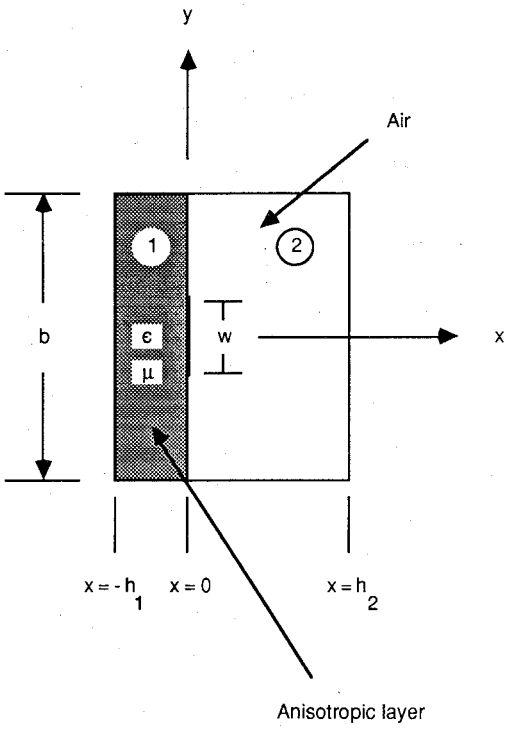

Fig. 1. Cross section of covered microstrip geometry.

where ϵ_0 and μ_0 denote the free-space values of the permittivity and permeability, respectively.

The spectral representation of the field may be obtained via the transform,

$$\tilde{\Phi}(x,\alpha)=\int_{-b/2}^{b/2}\Phi(x,y)e^{j\alpha y}\,dy \tag{2}$$

where α is the discrete transform variable, with values $\alpha=(2n-1)\pi/b$ allowed for E_z even–H_z odd modes and $\alpha=(2n\pi)/b$ restricted to the E_z odd–H_z even modes defined within the guide.

Maxwell's curl equations in the spectral space produce a pair of coupled second-order differential equations for $\tilde{E}_z$ and $\tilde{E}_y$. Decoupling of this set is possible and leads to yet another, but independent, pair of fourth-order equations for these components of the electric field, i.e.,

$$\frac{d^4}{dx^4}\tilde{E}_{z,y}+f_1\frac{d^2}{dx^2}\tilde{E}_{z,y}+f_2\tilde{E}_{z,y}=0 \tag{3a}$$

wherein the constants f_1 and f_2 are given by

$$f_1=k_0^2(\epsilon_{zz}\mu_{yy}+\epsilon_{yy}\mu_{zz})-\beta^2(\epsilon_{zz}/\epsilon_{xx}-\mu_{zz}/\mu_{xx})-\alpha^2(\mu_{yy}/\mu_{xx}+\epsilon_{yy}/\epsilon_{xx}) \tag{3b}$$

$$f_2=\left\{\left(k_0^2\mu_{yy}\epsilon_{zz}-\beta^2\epsilon_{zz}/\epsilon_{xx}-\alpha^2\mu_{yy}/\mu_{xx}\right)\cdot\left(k_0^2\mu_{zz}\epsilon_{yy}-\beta^2\mu_{zz}/\mu_{xx}-\alpha^2\epsilon_{yy}/\epsilon_{xx}\right)-(\alpha\beta)^2(\mu_{yy}/\mu_{xx}-\epsilon_{yy}/\epsilon_{xx})\cdot(\mu_{zz}/\mu_{xx}-\epsilon_{zz}/\epsilon_{xx})\right\}. \tag{3c}$$

The boundary conditions which require the tangential electric fields to vanish at the bottom (ground) plane $x=-h_1$ lead to the general solution to (3a), which in an anisotropic region may be written as

$$\tilde{E}_z^{\mathrm{I}}(x,\alpha)=A_n^*\sin\gamma_1^a(x+h_1)+B_n^*\sin\gamma_1^b(x+h_1) \tag{4a}$$

with the remaining transformed field components related to $\tilde{E}_z$ and $\tilde{E}_x$ in the following way:

$$\tilde{E}_y^{\mathrm{I}}(x,\alpha)=-(e_2)^{-1}\left\{(d^2/dx^2)\tilde{E}_z^{\mathrm{I}}(x,\alpha)+e_1\tilde{E}_z^{\mathrm{I}}(x,\alpha)\right\} \tag{4b}$$

$$\tilde{H}_z^{\mathrm{I}}(x,\alpha)=-(f_3)^{-1}\left\{\frac{d\tilde{E}_y^{\mathrm{I}}(x,\alpha)}{dx}+j\alpha\tilde{E}_x^{\mathrm{I}}(x,\alpha)\right\} \tag{4c}$$

$$\tilde{H}_y^{\mathrm{I}}(x,\alpha)=(f_4)^{-1}\left\{\frac{d\tilde{E}_z^{\mathrm{I}}(x,\alpha)}{dx}+j\beta\tilde{E}_x^{\mathrm{I}}(x,\alpha)\right\} \tag{4d}$$

$$\gamma_1^a,\gamma_1^b=\sqrt{\frac{f_1\pm\left(f_1^2-4f_2\right)^{1/2}}{2}}\,. \tag{4e}$$

$$e_1=k_0^2\mu_{yy}\epsilon_{zz}-\beta^2\epsilon_{zz}/\epsilon_{xx}-\alpha^2\mu_{yy}/\mu_{xx} \tag{4f}$$

$$e_2=\left(\frac{\mu_{yy}}{\mu_{xx}}-\frac{\epsilon_{yy}}{\epsilon_{xx}}\right)\alpha\beta. \tag{4g}$$

Note that the field component $\tilde{E}_x^{\mathrm{I}}$ can be determined by using two different methods. One way is to use the divergence equation, from which $\tilde{E}_x^{\mathrm{I}}$ is obtained by integrating the resulting equation after substituting for $\tilde{E}_y^{\mathrm{I}}$ and $\tilde{E}_z^{\mathrm{I}}$ into the expression for Gauss's law and then enforcing the appropriate boundary conditions at $x=0$. The other way is to use the curl equations, from which, after some manipulations, $\tilde{E}_x^{\mathrm{I}}$ can be expressed in terms of the derivatives of $\tilde{E}_y^{\mathrm{I}}$ and $\tilde{E}_z^{\mathrm{I}}$. Finally, the remaining terms appearing in (4) are the constants $f_3=(j\omega\mu_0\mu_{zz})^{-1}$ and $f_4=(j\omega\mu_0\mu_{yy})^{-1}$, γ_1^a and γ_1^b, which are separation constants in the x direction, and the corresponding modal amplitudes A_n^* and B_n^*.

The fields within the isotropic space, i.e., region 2, $\tilde{E}_z^{\mathrm{II}}(x,\alpha)$, $\tilde{E}_y^{\mathrm{II}}(x,\alpha)$, $\tilde{H}_z^{\mathrm{II}}(x,\alpha)$, and $\tilde{H}_y^{\mathrm{II}}(x,\alpha)$, are just a linear superposition of the TE and TM modes which have already been derived, and whose expressions are available in [9]. When boundary conditions are enforced at $x=0$ in the Fourier domain and are followed by some mathematical manipulations, they lead to a coupled equation set for the two current components $\tilde{J}_y$ and $\tilde{J}_z$:

$$\tilde{Z}_{zz}(\alpha,\beta)\tilde{J}_z(\alpha,\beta)+\tilde{Z}_{zy}(\alpha,\beta)\tilde{J}_y(\alpha,\beta)=\tilde{E}_{zs}(\alpha) \tag{5a}$$

$$\tilde{Z}_{yz}(\alpha,\beta)\tilde{J}_z(\alpha,\beta)+\tilde{Z}_{yy}(\alpha,\beta)\tilde{J}_y(\alpha,\beta)=\tilde{E}_{ys}(\alpha) \tag{5b}$$

where $\tilde{E}_{zs}$ and $\tilde{E}_{ys}$ are the tangential fields evaluated at the substrate–air boundary. In the above equations, the elements of the impedance matrix function can be expressed as

$$\tilde{Z}_{zz}(\alpha,\beta)=\tilde{Y}_{yy}(\alpha,\beta)/\Delta \tag{6a}$$

$$\tilde{Z}_{zy}(\alpha,\beta)=-\tilde{Y}_{zy}(\alpha,\beta)/\Delta \tag{6b}$$

$$\tilde{Z}_{yz}(\alpha,\beta)=-\tilde{Y}_{yz}(\alpha,\beta)/\Delta \tag{6c}$$

$$\tilde{Z}_{yy}(\alpha,\beta)=\tilde{Y}_{zz}(\alpha,\beta)/\Delta \tag{6d}$$

$$\Delta=\tilde{Y}_{yy}\tilde{Y}_{zz}-\tilde{Y}_{yz}\tilde{Y}_{zy} \tag{6e}$$

wherein the corresponding elements of the admittance matrix can be explicitly defined as

$$\tilde{Y}_{yy}(\alpha,\beta)=p_8\cot(\gamma_2h_2)-p_4\cot(\gamma_1^ah_1)/p_{11}+p_3\cot(\gamma_1^bh_1)/p_{11} \tag{7a}$$

$$\tilde{Y}_{zy}(\alpha,\beta)=+p_7\cot(\gamma_2h_2)+p_2\cot(\gamma_1^ah_1)/p_{10}-p_1\cot(\gamma_1^bh_1)/p_{10} \tag{7b}$$

$$\tilde{Y}_{yz}(\alpha,\beta)=+p_7\cot(\gamma_2h_2)+p_4p_5\cot(\gamma_1^ah_1)/p_{11}-p_3p_6\cot(\gamma_1^bh_1)/p_{11} \tag{7c}$$

$$\tilde{Y}_{zz}(\alpha,\beta)=p_9\cot(\gamma_2h_2)-p_2p_5\cot(\gamma_1^ah_1)/p_{10}+p_1p_6\cot(\gamma_1^bh_1)/p_{10}. \tag{7d}$$

The constants p appearing in (7) are given by

$$p_1 = \gamma_1^b + \beta(\alpha p_5 \epsilon_{yy}/\epsilon_{xx} + \beta\epsilon_{zz}/\epsilon_{xx})/\gamma_1^b \quad (8a)$$

$$p_2 = \gamma_1^a + \beta(\alpha p_6 \epsilon_{yy}/\epsilon_{xx} + \beta\epsilon_{zz}/\epsilon_{xx})/\gamma_1^a \quad (8b)$$

$$p_3 = -\alpha(\alpha p_5 \epsilon_{yy}/\epsilon_{xx} + \beta\epsilon_{zz}/\epsilon_{xx})/\gamma_1^b - p_5\gamma_1^b \quad (8c)$$

$$p_4 = -\alpha(\alpha p_6 \epsilon_{yy}/\epsilon_{xx} + \beta\epsilon_{zz}/\epsilon_{xx})/\gamma_1^a - p_6\gamma_1^a \quad (8d)$$

$$p_5 = \left((\gamma_1^b)^2 - e_1\right)/e_2 \quad (8e)$$

$$p_6 = \left((\gamma_1^a)^2 - e_1\right)/e_2 \quad (8f)$$

$$p_7 = \alpha\beta/\gamma_2 \quad (8g)$$

$$p_8 = \left(k_0^2 - \beta^2\right)/\gamma_2 \quad (8h)$$

$$p_9 = \left(k_0^2 - \alpha^2\right)/\gamma_2 \quad (8i)$$

$$p_{10} = (p_6 - p_5)/\mu_{yy} \quad (8j)$$

$$p_{11} = (p_6 - p_5)/\mu_{zz} \quad (8k)$$

where γ_2 denotes the separation constant in the x direction for region 2 and k_0 is the wavenumber of free space. Notice that $\tilde{E}_{zs}$ and $\tilde{E}_{ys}$ appearing in equations (5) are the unknowns at $x = 0$ for $w/2 < |y| < b/2$, but they are zero on the metal strip. As a result, a numerical solution to these equations can be obtained by using the technique which has been illustrated in [13]. The four unknowns contained therein are $\tilde{E}_{zs}$, $\tilde{E}_{zy}$, $\tilde{J}_z$, and $\tilde{J}_y$, where the former two can be eliminated by applying the Galerkin method in the Fourier domain. Specifically, to do this, the currents $\tilde{J}_y$ and $\tilde{J}_z$ are expanded in terms of basis functions $\tilde{J}_{ym}$ and $\tilde{J}_{zm}$, which in this case are chosen to be

$$\tilde{J}_z(n) = \sum_{m=1}^{N} sC_m \tilde{J}_{zm}(n) \quad (9a)$$

$$\tilde{J}_y(n) = \sum_{m=1}^{M} D_m \tilde{J}_{ym}(n) \quad (9b)$$

but where expansion constants C_m and D_m are still unknown. The basis functions must be taken such that they will satisfy the current boundary conditions; namely they must be singular at edges of the metal strip, i.e.,

$$J_{zm}(y) = \left[\cos\{2(m-1)\pi y/w\}\right] \Big/ \left[1-(2y/w)^2\right]^{1/2}, \quad m = 1,2,\cdots \quad (10a)$$

$$J_{ym}(y) = \left[\sin\{2(m)\pi y/w\}\right] \Big/ \left[1-(2y/w)^2\right]^{1/2}, \quad m = 1,2,\cdots. \quad (10b)$$

The matrix system can now be formed by substituting expansions (9) into equations (5) and taking the inner products with $\tilde{J}_{yi}$ and $\tilde{J}_{zi}$ for different values of the index i, so that the final form of these equations is given by

$$\sum_{m=1}^{N}\sum_{n=1}^{\infty} \tilde{J}_{zi}(n)\tilde{Z}_{zz}(n,\beta)\tilde{J}_{zm}(n)C_m + \sum_{m=1}^{M}\sum_{n=1}^{\infty} \tilde{J}_{zi}(n)\tilde{Z}_{zy}(n,\beta)\tilde{J}_{ym}(n)D_m = 0, \quad i = 1,2,\cdots,N \quad (11a)$$

$$\sum_{m=1}^{N}\sum_{n=1}^{\infty} \tilde{J}_{yi}(n)\tilde{Z}_{yz}(n,\beta)\tilde{J}_{zm}(n)C_m + \sum_{m=1}^{M}\sum_{n=1}^{\infty} \tilde{J}_{yi}(n)\tilde{Z}_{yy}(n,\beta)\tilde{J}_{ym}(n)D_m = 0 \quad i = 1,2,\cdots,M \quad (11b)$$

wherein the right-hand sides are zero by virtue of Parseval's theorem. Numerical solution of simultaneous equations (11) provides the propagation constant in the z direction, β, which is obtained by setting the determinant of the coefficient matrix equal to zero and searching for the root of the resulting equation.

III. Numerical Results

To validate the theory presented in this paper, effective dielectric constants are computed for two different types of substrates and are compared with previously published data. In the first case, the selected material is isotropic, with medium parameters $\epsilon_{xx} = \epsilon_{yy} = \epsilon_{zz} = 8.875$ and $\mu_{xx} = \mu_{yy} = \mu_{zz} = 1.0$; the physical dimensions of the waveguide housing and the strip are taken to be $b = 12.7$ mm, $h_1 = 1.27$ mm, $h_2 = 11.43$ mm, and $w = 1.27$ mm. A convergence check for this structure is performed by increasing the number of spectral terms as well as the matrix size. The computed data show that a matrix size as small as $M = N = 1$ and $n = 150$ terms yields a good result. Specifically, for this case the propagation constant β for $n = 250$ converges to its final value as 1.135615, 1.135451, 1.135450, and 1.135451 for $N = M = 1$, 2, 3, and 4, respectively. The corresponding values of the effective dielectric constant when $N = M = 1$ and $n = 250$ are shown in Fig. 2 versus frequency ranging from dc to 20.0 GHz. The data from [13] are also reproduced to show that good agreement is obtained, which is expected since the Green's function used in [13] and [14] is exactly identical to the one presented here when it reduces to the isotropic case. Also shown in this figure is another comparison between results computed by the present method and those obtained via the hybrid mode technique [7]. In this case, sapphire is used as a substrate for the microstrip. For this material, the relative permittivity and permeability parameters are $\epsilon_{xx} = 11.6$, $\epsilon_{yy} = \epsilon_{zz} = 9.4$, and $\mu_{xx} = \mu_{yy} = \mu_{zz} = 1.0$, respectively. The effective dielectric constant, ϵ_{eff}, is once again computed versus frequency for up to 50.0 GHz, and excellent agreement between the two methods is observed throughout the selected frequency range.

The computations are then extended to the microstrip line on a dielectrically biaxial material, with the substrate being the PTFE cloth. The corresponding geometrical parameters of the structure are chosen as $b = 12.7$ mm, $h_1 = 0.50$ mm, and $h_2 = 12.20$ mm and the substrate material is characterized by $\epsilon_{xx} = 2.45$, $\epsilon_{yy} = 2.89$, $\epsilon_{zz} = 2.95$, and $\mu_{xx} = \mu_{yy} = \mu_{zz} = 1.0$. For this type of cloth, Fig. 3 shows the behavior of ϵ_{eff} for different w/h_1 ratios as the frequency increases up to 50.0 GHz and where the effective dielectric constant exhibits only a small variation over the computed frequency band. On the other hand, for the glass cloth, which is characterized by $\epsilon_{xx} = 6.24$, $\epsilon_{yy} = 6.64$, and $\epsilon_{zz} = 5.56$, ϵ_{eff} is noticeably more sensitive to changes in the frequency, and as a result it varies more rapidly than in the previous case of the PTFE cloth, as indicated in Fig. 4.

To illustrate the general applicability of the approach presented in this paper, the propagation constant β ($\beta^2 = \epsilon_{\text{eff}} k_0^2$) of the microstrip line printed on a substrate that is characterized by $\epsilon_{xx} = 2.0$, $\epsilon_{yy} = 2.35$, and $\epsilon_{zz} = 3.5$ and several different combinations of the tensor elements of $[\mu]$ is presented in Fig. 5. The curves are generated to show explicitly the magnetic anisotropy effects on the propagation constant. For values of μ_{xx}, μ_{yy}, and μ_{zz} increasing from 2.75, 2.25, 5.0 to 4.25, 3.75, 6.5, as indicated by letters A through D in Fig. 5, the calculated propagation constant β is clearly sensitive to variations in ele-

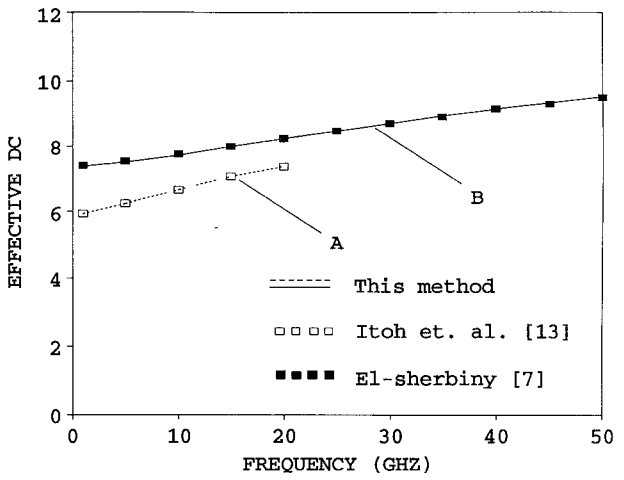

Fig. 2. Effective dielectric constant versus frequency. A: Isotropic with $b = 12.7$ mm, $h_1 = 1.27$ mm, $h_2 = 11.43$ mm, $w = 1.27$ mm, $\epsilon_{xx} = \epsilon_{yy} = \epsilon_{zz} = 8.875$, and $\mu_{xx} = \mu_{yy} = \mu_{zz} = 1.0$. B: Sapphire with $w/h_1 = 1.0$, $h_1 = 0.5$ mm, $\epsilon_{xx} = 11.6$, $\epsilon_{yy} = \epsilon_{zz} = 9.4$, and $\mu_{xx} = \mu_{yy} = \mu_{zz} = 1.0$.

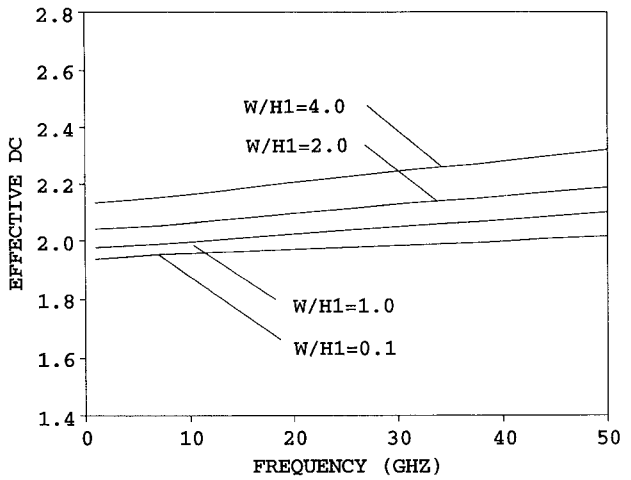

Fig. 3. Effective dielectric constant versus frequency of a line on PTFE cloth with $b = 12.70$ mm, $h_1 = 0.50$ mm, $h_2 = 12.20$ mm, $\epsilon_{xx} = 2.45$, $\epsilon_{yy} = 2.89$, $\epsilon_{zz} = 2.95$, and $\mu_{xx} = \mu_{yy} = \mu_{zz} = 1.0$.

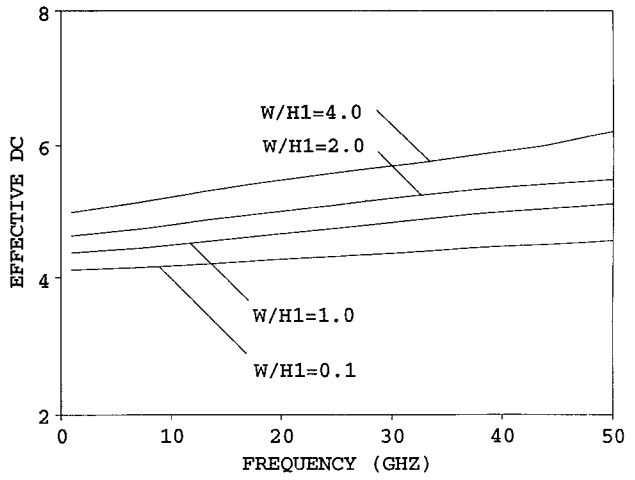

Fig. 4. Effective dielectric constant versus frequency of a line on glass cloth with $b = 12.70$ mm, $h_1 = 0.50$ mm, $h_2 = 12.20$ mm, $\epsilon_{xx} = 6.24$, $\epsilon_{yy} = 6.64$, $\epsilon_{zz} = 5.56$, and $\mu_{xx} = \mu_{yy} = \mu_{zz} = 1.0$.

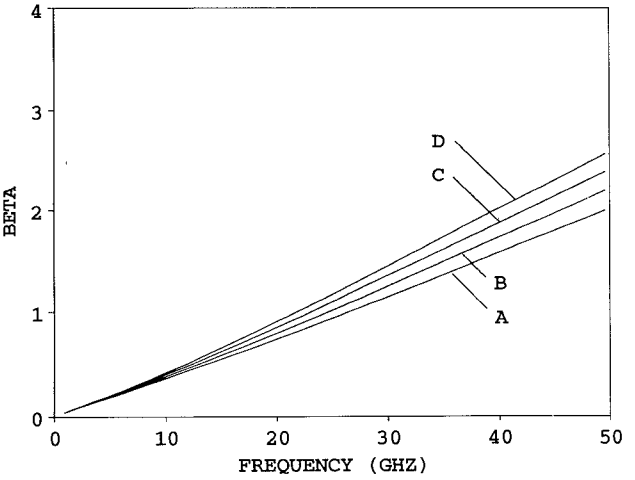

Fig. 5. Propagation constant versus frequency with $b = 12.70$ mm, $h_1 = 0.50$ mm, $h_2 = 12.20$ mm, $w = 0.500$ mm, $\epsilon_{xx} = 2.0$, $\epsilon_{yy} = 2.35$, and $\epsilon_{zz} = 3.50$. A: $\mu_{xx} = 2.75$, $\mu_{yy} = 2.25$, and $\mu_{zz} = 5.00$. B: $\mu_{xx} = 3.25$, $\mu_{yy} = 2.75$, and $\mu_{zz} = 5.50$. C: $\mu_{xx} = 3.75$, $\mu_{yy} = 3.25$, and $\mu_{zz} = 6.00$ D: $\mu_{xx} = 4.25$, $\mu_{yy} = 3.75$, and $\mu_{zz} = 6.50$.

ments of $[\mu]$ beyond the frequency of 12.50 GHz. Results of Fig. 5 reaffirm the fact that, as expected, the anisotropy effects, whether electric or magnetic, are amplified at higher frequencies and must be taken into account in the design of high-frequency circuits.

As a final note, it should be added that all calculations of the data presented in this paper were carried out by using the 25 MHz AT-compatible 486 PC. Typical computation times for a single frequency point using 250 spectral terms are 2.7 s, 3.0 s, 3.5 s, and 3.9 s respectively for matrix sizes of $N = M = 1$, $N = M = 2$, $N = M = 3$, and $N = M = 4$, which demonstrates the practicality of the spectral-domain method in the numerical analysis of MIC's.

IV. Conclusion

The spectral-domain method has been applied to an analysis of a shielded microstrip line on a biaxial anisotropic substrate which takes into account both dielectric and magnetic anisotropy effects, which are very important in high-frequency applications. The characteristic equation for the propagation constant used to obtain ϵ_{eff} is formed by applying the Galerkin technique in the Fourier domain. The calculated effective dielectric constants for two special validation cases are shown to be in good agreement with those computed using other methods. To demonstrate the versitility of this approach, numerical results for the microstrip line on a substrate that is characterized simultaneously by different $[\epsilon]$ and $[\mu]$ are presented which clearly convey the importance of all tensor parameters, especially when MIC's operate at higher frequencies.

Acknowledgment

The authors wish to thank Dr. Y. C. Shih from Hughes Industrial Electronics Group for his valuable suggestions toward this work.

References

[1] R. P. Owens, J. E. Itken, and T. C. Edwards, "Quasi-static characteristics of microstrip on an anisotropic sapphire substrate," *IEEE Trans. Microwave Theory Tech.*, vol. MTT-24, pp. 499–505, Aug. 1976.

[2] T. C. Edwards and R. P. Owens, "2–18 GHz dispersion measurements on 10–100 Ω microstrip lines on sapphire," *IEEE Trans. Microwave Theory Tech.*, vol. MTT-24, pp. 506–513, Aug. 1976.
[3] N. G. Alexopoulos and C. M. Krowne, "Characteristics of single and coupled microstrips on anisotropic substrates," *IEEE Trans. Microwave Theory Tech.*, vol. MTT-26, pp. 387–393, June 1978.
[4] N. G. Alexopoulos, "Integrated-circuit structures on anisotropic substrates," *IEEE Trans. Microwave Theory Tech.*, vol. MTT-33, pp. 847–881, Oct. 1985.
[5] M. Horno, "Quasistatic characteristics of microstrip on arbitrary anisotropic substrates," *Proc. IEEE*, vol. 67, pp. 1033–1034, Aug. 1980.
[6] S. K. Koul and B. Bhat, "Inverted microstrip and suspended microstrip with anisotropic substrates," *Proc. IEEE*, vol. 70, pp. 1230–1231, Oct. 1982.
[7] A-M. A. El-Sherbiny, "Hybrid mode analysis of microstrip lines on anisotropic substrates," *IEEE Trans. Microwave Theory Tech.*, vol. MTT-29, pp. 1261–1265, Dec. 1981.
[8] M. Kobayashi, "Frequency dependent characteristics of microstrips on anisotropic substrates," *IEEE Trans. Microwave Theory Tech.*, vol. MTT-30, pp. 2054–2057, Nov. 1982.
[9] H. Yang and N. G. Alexopoulos, "Uniaxial and biaxial substrate effects on finline characteristics," *IEEE Trans. Microwave Theory Tech.*, vol. MTT-35, pp. 24–29, Jan. 1987.
[10] C. M. Krowne, A. A. Mostafa, and K. A. Zaki, "Slot and microstrip guiding structures using magnetoplasmons for nonreciprocal millimeter-wave propagation," *IEEE Trans. Microwave Theory Tech.*, vol. 36, pp. 1850–1860, Dec. 1988.
[11] G. E. Mariki and C. Yeh, "Dynamic three-dimensional TLM analysis of microstriplines on anisotropic substrate," *IEEE Trans. Microwave Theory Tech.*, vol. MTT-33, pp. 789–799, Sept. 1985.
[12] J. L. Tsalamengas, N. K. Uzunoglu, and N. G. Alexopoulos, "Propagation characteristics of a microstrip line printed on a general anisotropic substrate," *IEEE Trans. Microwave Theory Tech.*, vol. MTT-33, pp. 941–945, Oct. 1985.
[13] T. Itoh and R. Mittra, "A technique for computing dispersion characteristics of shielded microstrip lines," *IEEE Trans. Microwave Theory Tech.*, vol. MTT-22, pp. 896–898, Oct. 1974.
[14] T. Itoh, "Analysis of microstrip resonators," *IEEE Trans. Microwave Theory Tech.*, vol. MTT-22, pp. 946–952, Nov. 1974.

Frequency-Dependent Characteristics of Shielded Broadside Coupled Microstrip Lines on Anisotropic Substrates

T. Q. Ho and B. Beker

Abstract—**In this paper, a spectral-domain technique is applied to compute the propagation characteristics of a shielded broadside coupled microstrip line printed on homogeneous uniaxial and biaxial substrates. The formulation derives the Green's functions for even and odd modes of the guiding structure via the transformed fourth-order differential equations. The analysis includes anisotropic substrates which are simultaneously characterized by both $[\epsilon]$ and $[\mu]$ tensors. This rigorous full-wave approach to the solution of the problem is shown to yield results agreeing well with the existing data. The propagation characteristics are studied with respect to different line width/thickness ratios as well as to the material substrate parameters.**

Manuscript received October 15, 1990; revised January 15, 1991.
The authors are with the Department of Electrical and Computer Engineering, University of South Carolina, Columbia, SC 29208.
IEEE Log Number 9144277.

I. Introduction

Among the various E-plane transmission line structures available for practical applications at microwave and millimeter-wave frequencies, the broadside coupled microstrip line is one of the most commonly used. In order to accurately design MIC circuits using this structure, the effect of dispersion should be carefully considered. One of the first studies of a broadside coupled microstrip line on isotropic substrates was carried out by Allen *et al.* [1]. Subsequently, Bornemann [2] also examined the dispersion characteristics of similar structures, however, without providing numerical results for the even-mode case. More recently, Mizuno *et al.* [3] have studied the same structure using a rigorous analysis to calculate dispersion properties of both the even and odd modes.

While isotropic media are frequently employed as substrates in circuits of this type, at higher frequency they may exhibit anisotropic properties as well. To account for such effects, D'Assunçaso *et al.* [5] have used the method of moments to study the broadside coupled line with no sidewalls on anisotropic substrates. However, this approach is quasi-static, so the results are limited to low frequencies. As an alternative, Koul *et al.* [6] presented a technique which is based on the transverse transmission line method for analyzing broadside coupled circuits of this kind using anisotropic media. Unfortunately, in all of the aforementioned works, the formulation of the problem considered materials characterized by tensor permittivity alone, and, in some cases, the analysis was further restricted to uniaxial substrates.

In this paper, the spectral-domain method is extended to study a shielded broadside coupled microstrip line along the E plane of the waveguide printed on anisotropic medium. The problem is generalized so that both dielectric and magnetic anisotropy effects are included in the formulation. The analysis is rigorously performed so that accurate full-wave solutions may be obtained. The two transformed fourth-order differential equations, which can be obtained from Maxwell's curl equations, yield solutions that lead to the derivation of the Green's functions for both the even- and the odd-mode case. The characteristic equation for the propagation constant is formed by applying the Galerkin method in the Fourier transform domain. Numerical results for the broadside coupled line are computed for a special isotropic case and are compared with the ones obtained in [3]. Good agreement for the effective dielectric constant is observed in the computed data throughout the selected w/b (strip-guide width) range. Additional examples exhibiting the behavior of the effective dielectric and propagation constants of the line on various anisotropic substrates including sapphire, boron nitride, filled PTFE (glass cloth), PTFE cloth, and lithium niobate are also presented.

II. Formulation

The broadside coupled microstrip line structure, shown in Fig. 1(a), consists of a thin substrate material layer characterized by both $[\epsilon]$ and $[\mu]$ biaxial tensors which is suspended inside a metal housing with dimensions a and b. The substrate, of thickness $2h_1$, is assumed to be lossless and is uniformly extended in the z direction. To simplify the analysis, the metal strips whose width is w are also assumed to be perfectly conducting and infinitely thin in the x direction. The medium properties of the substrate are characterized by diagonal biaxial

0018-9480/91/0600-1021$01.00 ©1991 IEEE